Automatic Path Planning for Welding Robot Based on Reconstructed Surface Model

Wusheng Chou, Liang You, and Tianmiao Wang

Robotics Institute, Beijing University of Aeronautics and Astronautics,
Beijing, 100083, P.R. China
wschou@buaa.edu.cn

Abstract. An automatic path planning method, including the torch pose planning, is proposed to improve the flexibility and automatic planning ability of arc welding robot. The virtual object, which representing the real object to be welded, is reconstructed firstly by non-rational B-spline surface from geometric polygonal mesh model or measured point cloud. Based on the reconstructed non-rational surface model, the tangent vector and the tangent plane of each sampling point on the space welding seam is calculated, as well as the normal plane of each sampling point. Thus the position and pose of torch with respect to each sampling point of space seam can be determined by the calculated tangent vector, normal plane and concrete requirement of welding process. The final path planning of arc welding robot in joint space is obtained by its inverse kinematics. Experimental results demonstrate the accuracy and the feasibility of the proposed method.

1 Introduction

Welding robot play an important role in improving the quality and productivity of industrial manufacturing. Generally speaking, the on-line teaching method and the off-line programming method are adopted to generate suitable robot program to perform welding task [1]. On line teaching method can fully utilize the intelligence of human operator, but it is time consuming and lowly efficient for complex space welding seam [2]. The more profitable method of building a work program is to use off-line programming, which is easy to verify the validity of the robot programs through simulation and visualization.

The working process of welding robot consists of welding procession and motion process [3]. The path planning of welding robot is similar as traditional robot motion planning, and some work focus on obstacle avoidance, shortest time and shortest path [4]. Genetic Algorithm is used to generate optimal robot traveling path [5]. Machine vision is also often used to track seam and plan path [6]. Due to the low quality image in welding process, it is hard to recognize and extract useful information from the feedback image. With the development of virtual reality and CAD technology, some off-line programming and path planning methods are proposed. The three dimensional problem of planning of arc welding torch's gesture is translated into a two dimensional problem in the plane of welding torch location [7]. This method is suitable to linear seam and not easy to deal with space seam. The position and posture file of welding torch is generated from a three dimension solid model [8], and the torch plane is determined by the normal of the vertex of triangular polygon. However, the normal of

T.-J. Tarn et al. (Eds.): Robot. Weld., Intellige. & Automation, LNCIS 362, pp. 153–161, 2007.
springerlink.com

the vertex of triangular polygon is not the real normal of the surface at the vertex, and the tangent vector at the vertex can not be determined. There is also a trade-off between the accuracy and the approximation of solid object using polygonal model. Precise approximations increase the complexity of the boundary representation. On the other hand, a small number of polygons compromise the quality or even the correctness of the simulation.

We propose a new method to automatically generate welding path by decomposing the path planning of welding robot into torch pose planning and trajectory planning in joint space. Firstly we reconstruct the welded object using B-spline surface model, which can fit the given point cloud of geometric model with high precision. The torch plane perpendicular to the tangent vector of seam can be easily obtained accurately by analytic operation, which is the most important base to determine the torch pose according to the requirement of welding process. The trajectory of welding robot in joint space is so generated by inverse kinematics.

The rest of this paper is organized as follows. Section 2 describes the algorithm to reconstruct the B-spline surface model. The posture and position planning of torch is presented in Section 3, and Section 4 gives some experimental results. Section 5 concludes the paper.

2 Adaptive Fitting Algorithm of B-Spline Surface

The key process of object reconstruction is to fit the virtual object to given point set. Surface fitting of spheres, cylinders, cones and tori can be obtained by least square method [9]. Non rational B-spline can be used for surface fitting with C2 continuity and good performance [10]. However, the noise and cog of the characteristic points bring non-neglected fitting errors in non rational B-spline based method. Here we develop an adaptive surface fitting algorithm to fit the given point cloud with high accuracy. The given point cloud can be obtained from CAD geometric polygonal model or from laser measurement.

2.1 Selection of Parametric Direction and Knot Vector

The points obtained from complex surface can be arranged in a topological rectangular array with the elements $p_{i,j}(i=0,1,\cdots,r;\ j=0,1,\cdots,s)$. Let u denote the horizontal direction, then v denotes vertical direction. If all the points in the same row or column lie in a plane, then we select the group of curve obtained by interpolated among these points to be the dissection face curve with parameter u and v. There are s+1 horizontal dissection face points. The horizontal and vertical knot vector can be obtained by making the arc length parametric along the u and v directions. The parameters $(\tilde{u}_i, \tilde{v}_j)$ correspond to the point $q_{i,j}$. So the reconstructed surface description can be written as

$$p(u,v)=\sum_{i=0}^{m}\sum_{j=0}^{n} d_{i,j}N_{i,3}(u)N_{j,3}(v),\quad 0\le u,v\le 1 \tag{1}$$

Where the knot vector in u and v direction are $U=[u_0,u_1,\cdots,u_{m+4}]$ and $V=[v_0,v_1,\cdots,v_{n+4}]$, respectively. The definition area of surface are $u\in[u_3,u_{m+1}]=[0,1]$, $v\in[v_0,v_{n+1}]=[0,1]$. The parameter corresponding to point $q_{i,j}$ is

$$(u_i,v_j)=(\tilde{u}_{i-3},\tilde{v}_{j-3})\ (i=3,4,\cdots,m+1;\ j=3,4,\cdots,n+1) \tag{2}$$

Where m=r+2, n=s+2.

On the other hand, there are two cases for the star and end points along the u,v directions. The first one is that the star and end points along u or v direction overlay each other and it is C2 closed surface. In this case, the knot which is beyond knot vector U can be determined as

$$u_0=u_{m-2}-1,u_1=u_{m-1}-1 \tag{3}$$

$$u_2=u_m-1,u_{m+2}=1+u_4,u_{m+3}=1+u_5,u_{m+4}=1+u_6 \tag{4}$$

The second one is that although the star and end points along u or v direction overlay each other, but the surface is open. The knot which is beyond knot vector U can be determined as

$$u_0=u_1=u_2=u_3=0 \tag{5}$$

$$u_{m+1}=u_{m+2}=1,u_{m+3}=u_{m+4}=1 \tag{6}$$

2.2 Calculation of the Control Points of Three Order B-Spline Surface

According to the properties of tensor product surface, equation (1) can be rewritten as

$$p(u,v)=\sum_{i=0}^{m}\left(\sum_{j=0}^{n}d_{i,j}N_{j,3}(v)\right)N_{i,3}(u)=\sum_{i=0}^{m}c_i(v)N_{i,3}(u) \tag{7}$$

where there are m+1 points on the control curves with parameter v_j, which can be represented as

$$c_i(v)=\sum_{j=0}^{n}d_{i,j}N_{j,3}(v)(\ i=0,1,\cdots,m) \tag{8}$$

In the case that the conjunction of the start and the end of a closed surface is not C2 continuity, or the curve is open along some parameter, the $m+2$ unknown control points cannot be calculated by solving the equation group consisting of m-1 equations, according to the r+1 = m-1 points along u direction. Some end conditions should be

derived to get two additional equations. The end conditions can be determined by the tangent vector along *u* and *v* parameters.

2.3 Adaptive Algorithm of Three Order B-Spline Surface Fitting

The reconstructed B-spline surface can be defined by the calculated control points $d_{i,j}(i=0,1,\cdots,m;\ j=0,1,\cdots,n)$ and the obtained knot vectors $U=[u_0,u_1,\cdots,u_{m+4}]$ and $V=[v_0,v_1,\cdots,v_{n+4}]$. Due to the noise and cog of measured points, there will be error between the reconstructed surface and the original surface. The limit of error E is

$$\delta=\left|q_{i,j}-p(\tilde{u}_i,\tilde{v}_j)\right|\ \ (i=0,1,\cdots,r\,;\ j=0,1,\cdots,s) \tag{9}$$

If the point on the reconstructed surface with parameters $(\tilde{u}_i,\tilde{v}_j)$ has larger error, the corresponding control point should be adjusted to fit the original points better by moving the control point $d_{i,j}$ to a new position $d^*_{i,j}$ along the connection line of point $q_{i,j}$ and point $p(\tilde{u}_i,\tilde{v}_j)$.

So we can obtain

$$\alpha=\delta/(|\,c\,|\,N_{i,3}(u_i)N_{j,3}(v_j)) \tag{10}$$

Thus the new control point $d^*_{i,j}$ can be obtained by the following equation

$$d^*_{i,j}=d_{i,j}+\alpha c \tag{11}$$

3 Automatic Path Planning

For robotic welding system, the end of torch is constrained by the seam. Generally, there is a small distance *D* between the end of torch and the seam, and there is a tilting angle θ between the tangent vector and the torch.

As shown in Fig.1, the tangent plane and tangent vector of sampling point Ps on space seam can be easily calculated according to the parametric description of the reconstructed B-spline surface. Thus we can get the normal plane passing through the sampling point of the space seam according to the tangent vector. The normal plane at Ps is the basic knowledge for torch pose and position planning. For example, if the welding process requires that the torch locates in the normal plane, then a new direction V can be obtained which is the z axis of the torch and has a crossing angle θ with respect to the tangent vector in the normal plane. The position of the end of the torch can also be obtained by offsetting Ps a distance D along the new direction V.

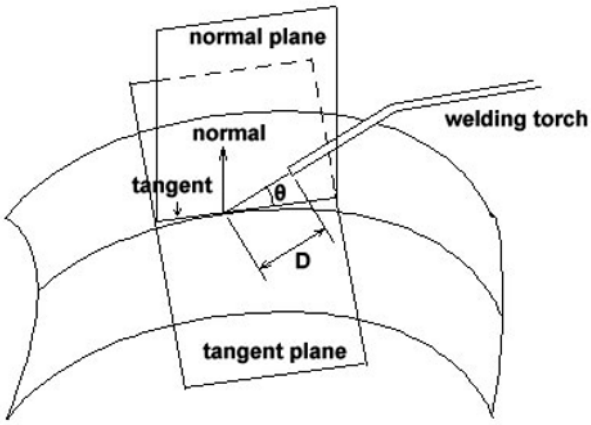

Fig. 1. The Determination of Torch Position and Pose

4 Experimental Results

The accuracy of surface fitting based on B spline is tested firstly. Given a set of scattered point cloud (1000 points) of a sphere whose radius is 100 units, the virtual sphere is reconstructed with parametric descriptions. The error between the original point and their corresponding point on the reconstructed sphere surface is shown as Fig.2. The average error is 0.02 unit and the maximum error is 0.4 unit with respect to the sphere radius of 100 units.

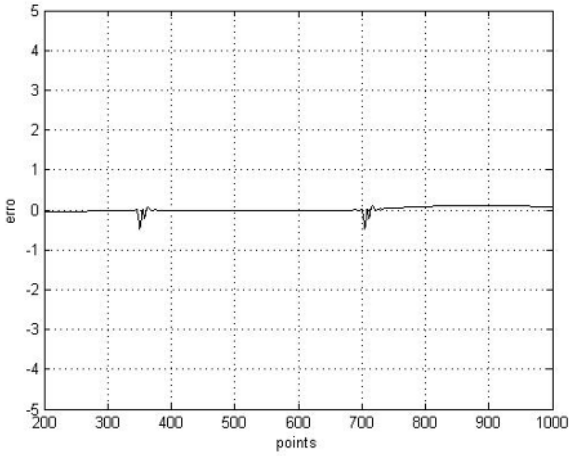

Fig. 2. The Error between the Ooriginal Point and Their Corresponding Point on the Reconstructed Surface

Two space seams are given then to testify the feasibility of the proposed automatic path planning method. One is a circle seam on a sphere with a radius of 90 units, and another one is a S shaped seam which is on a vertical plane. Our method works well with these cases. The positions of the end of the torch after automatic planning are shown as Fig.3 and Fig.4,repectively, while satisfying the requirement that the torch locates in the normal plane of the sampling points of the these space seams and have a cross angle of 30 degree with the tangent vector.

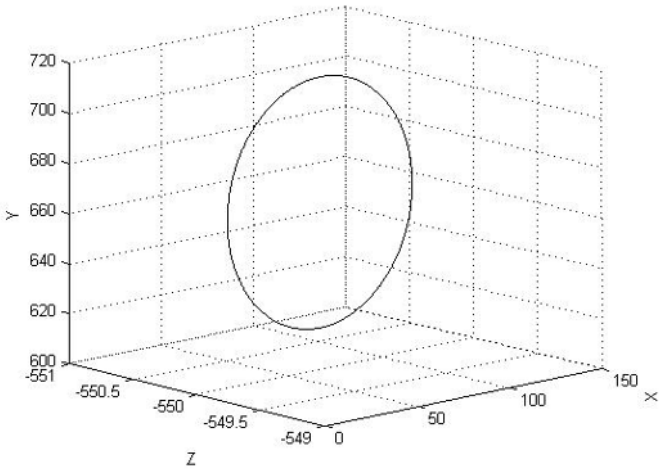

Fig. 3. Automatically Planned Path of the Torch for a Circle Seam

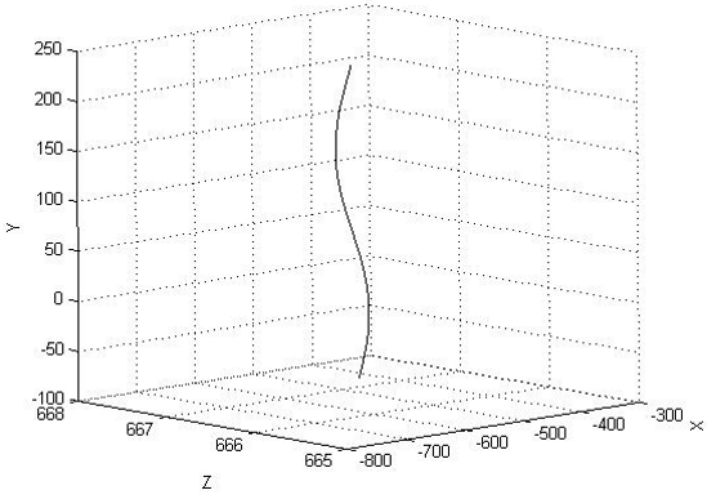

Fig. 4. Automatically Planned Path of the Torch for a S Shaped Vertical Seam

The trajectories of the 6 DOF welding robot, whose kinematics is described by equation (12), are shown as Fig. 5 and Fig.6, respectively, when the end of torch moving along the circle seam in clockwise and moving along the perpendicular seam from top to down. From Fig.5 and Fig.6, it can be seen that the trajectories of the joints are very smooth while the robot conduct welding task. Since the reconstructed surface is third order continuity, it also avoids the disadvantages of polygonal mesh model, which can cause joint jog.

$$
\begin{aligned}
A1&=\begin{bmatrix} \cos\theta_1 & -\sin\theta_1 & 0 & 0 \\ \sin\theta_1 & \cos\theta_1 & 0 & 0 \\ 0 & 0 & 1 & 330.2 \\ 0 & 0 & 0 & 1 \end{bmatrix} \quad A2=\begin{bmatrix} \cos\theta_2 & -\sin\theta_2 & 0 & 0 \\ 0 & 0 & 1 & 67 \\ -\sin\theta_2 & -\cos\theta_2 & 0 & 0 \\ 0 & 0 & 0 & 1 \end{bmatrix} \\
A3&=\begin{bmatrix} \cos\theta_3 & -\sin\theta_3 & 0 & 198.1 \\ \sin\theta_3 & \cos\theta_3 & 0 & -19.1 \\ 0 & 0 & 1 & 55 \\ 0 & 0 & 0 & 1 \end{bmatrix} \quad A4=\begin{bmatrix} \cos\theta_4 & -\sin\theta_4 & 0 & 0 \\ 0 & 0 & -1 & -207.1 \\ \sin\theta_4 & \cos\theta_4 & 0 & 0 \\ 0 & 0 & 0 & 1 \end{bmatrix} \\
A5&=\begin{bmatrix} \cos\theta_5 & -\sin\theta_5 & 0 & 0 \\ 0 & 0 & -1 & 0 \\ -\sin\theta_5 & -\cos\theta_5 & 0 & 0 \\ 0 & 0 & 0 & 1 \end{bmatrix} \quad A6=\begin{bmatrix} \cos\theta_6 & -\sin\theta_6 & 0 & 0 \\ 0 & 0 & -1 & -132.5 \\ \sin\theta_6 & \cos\theta_6 & 0 & 0 \\ 0 & 0 & 0 & 1 \end{bmatrix} \\
A7&=\begin{bmatrix} 1 & 0 & 0 & 0 \\ 0 & 1 & 0 & 0 \\ 0 & 0 & 1 & 203 \\ 0 & 0 & 0 & 1 \end{bmatrix}
\end{aligned} \tag{12}
$$

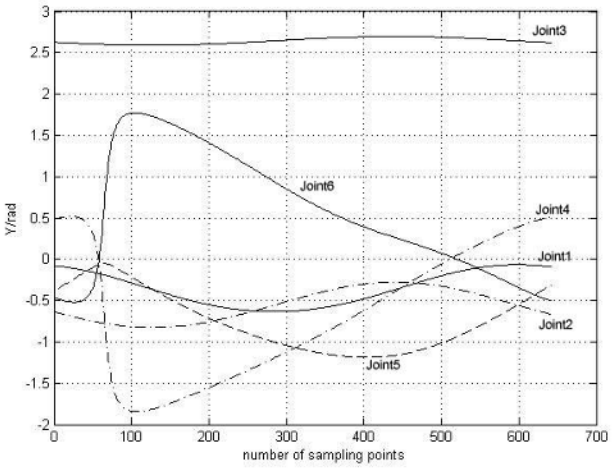

Fig. 5. Trajectories of Robot Joints for Space Circle Seam

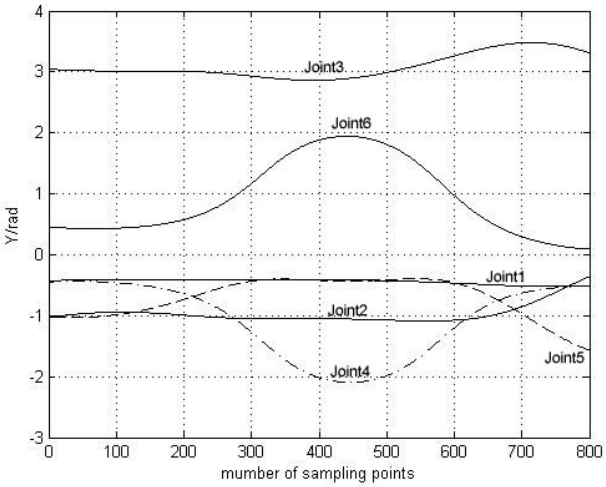

Fig. 6. Trajectories of Robot Joints for Space Vertical Seam

5 Conclusion

Based on the reconstructed parametric surface, an automatic path planning method is proposed. The surface fitting algorithm in this paper can also deal with the noise and cog of given points, and the virtual object can be reconstructed by three order B-spline surface with high accuracy. Through analytic calculation of the reconstructed parametric surface, the tangent vector as well as the normal plane at the sampling points of space seam can be easily obtained, which provide a basic reference for the determination of poison and torch pose according to concrete requirement of welding process. Another advantage of the proposed method is that the joint trajectories are smooth, since the automatically planned positions of the end of torch are on smooth surface instead of polygonal mesh model. Our future work is to automatically generate the robot program after path planning and to perform real welding task via augmented reality.

Acknowledgement

The authors are grateful to the support of National Science Foundation of China under grants 60525314 and the support of the National Key Basic Research Program (973 program) under grant 2002CB312200.

References

1. Ulrich D (1992) Robot systems for arc welding - current position and future trends. Welding and Cutting (8): 150-152
2. Regev Yocam (1995) The evolution of off line programming. Industrial Robot 22(3): 5-7

3. Breat JL, Clement F, Jadeau P, et al. (1994) ACT WELD - an unique off-line programming software tailored for robotic welding applications. Welding in the World 34 (3):267-274.
4. Chen Q, Lu J, Sun Z, et al. (2002) Study on torch pose planning system for arc welding robot. Chinese Mechanical Engineering 13(11):956-958.
5. Hong KS, Han HY (2004) PC Based off line programming using VRML for welding robots in shipbuilding. IEEE International Conference on Robotics, Automation and Mechatronics: 949-954,
6. Peng J, Chen Q, Lu J, et al. (1998) Real time optimization of robotic arc welding based on machine vision and neural networks. Proceeding of 24th Annual Conf of IECON : 1279-1283.
7. Zhu DL, Xiao S, Hou H, et al. (2004) Automatic planning of welding torch's gesture of arc welding robot. Journal of Shanhai Jiaotong University 38(9): 1472-1475,
8. Yan H, Liu J, Qiu SH, et al. (2005) Research on the automatic planning of arc welding robot welding path for space weld. Machinery Design and Manufacturing (8):106-106,
9. Lukács G, Marshall AD, Martin RR (1998) Faithful least-squares fitting of spheres, cylinders, cones and tori for reliable segmentation. Proc ECCV 98, Lecture Notes in Computer Science, Springer (1):6712